

Evidence from Mechanistic Probes for Distinct Hydroperoxide Rearrangement Mechanisms in the Intradiol and Extradiol Catechol Dioxygenases

Meite Xin and Timothy D. H. Bugg*

Department of Chemistry, University of Warwick, Coventry CV4 7AL, U.K.

Received April 22, 2008; E-mail: T.D.Bugg@warwick.ac.uk

Abstract: Three mechanistic probes were used to investigate whether the Criegee rearrangement step of catechol 1,2-dioxygenase (CatA) from *Acinetobacter* sp. proceeds via a direct 1,2-acyl migration, via homolytic O—O cleavage, or via a benzene oxide—oxepin rearrangement. Incubation of CatA with 3-chloroperoxybenzoic acid led to the formation of a 9:1 mixture of 2-chlorophenol and 3-chlorophenol, via a mechanism involving O—O homolytic cleavage. Incubation of CatA with 2-hydroperoxy-2-methylcyclohexanone led to formation of 5,6-diketoheptan-1-ol, also consistent with an O—O homolytic cleavage mechanism, and not consistent with a direct 1,2-acyl migration. No reaction product was isolated from incubation of CatA with 6-hydroxymethyl-6-methylcyclohexa-2,4-dienone, an analogue that is able to undergo the benzene oxide—oxepin rearrangement, but not able to undergo O—O homolytic cleavage. In contrast, incubation of extradiol dioxygenase MhpB from *Escherichia coli* with 6-hydroxymethyl-6-methylcyclohexa-2,4-dienone led to the formation of a 2-tropolone ring expansion product, consistent with a direct 1,2-alkenyl migration for extradiol cleavage. Taken together, the results imply different mechanisms for the Criegee rearrangement steps of intradiol and extradiol catechol dioxygenases: a direct 1,2-alkenyl migration for extradiol cleavage and an O—O homolytic cleavage mechanism for intradiol cleavage.

Introduction

The nonheme iron-dependent catechol dioxygenases catalyze the oxidative cleavage of catechol substrates as part of aromatic degradation pathways found in soil bacteria.^{1,2} The intradiol catechol dioxygenases, containing a mononuclear iron(III) cofactor ligated by two tyrosine and two histidine residues, generate a muconic acid product, whereas the extradiol catechol dioxygenases, containing a mononuclear iron(II) cofactor ligated by two histidine and one glutamic acid residue, generate a 2-hydroxymuconaldehyde product.

A long-standing question in the study of these enzymes has been: what factors control the choice of intradiol vs extradiol reaction specificity?³ The initial steps of substrate/dioxygen activation are different: the iron(III) center of the intradiol dioxygenases is believed to activate the substrate catecholate dianion for reaction with dioxygen,² as a high-spin iron(III) catecholate complex with strong π -character,⁴ while the iron(II) center of the extradiol dioxygenases is believed to activate dioxygen as superoxide to react with a catecholate monoanion.⁵ In both cases, however, the same proximal hydroperoxide intermediate is formed, and this intermediate has been observed directly by protein crystallography in homoprotocatechuate 2,3-dioxygenase (2,3-HPCD) from *Brevibacterium fuscum*.⁶ This

hydroperoxide undergoes different Criegee rearrangements in the two classes of enzyme, as shown in Figure 1: the intradiol dioxygenases catalyze a 1,2-acyl migration to form an anhydride intermediate, while the extradiol dioxygenases catalyze a 1,2-alkenyl migration to form a lactone intermediate.³

The 1,2-alkenyl migration of the extradiol dioxygenases is assisted by acid–base catalysis by active-site histidine residues,⁷ whereas the active sites of the intradiol dioxygenases contain no outer sphere acid–base residues. Extensive model chemistry on catechol cleavage by iron complexes has shown that intradiol cleavage can be catalyzed by a wide range of tripodal tetradentate iron(III) complexes,⁸ while extradiol cleavage is only observed in a small number of complexes with facial, tridentate ligands;^{9,10} hence, the coordination chemistry of the iron center clearly influences its reactivity, but exactly how the choice of acyl vs alkenyl migration is controlled is not clear.

The 1,2-acyl migration rearrangement in the intradiol catechol dioxygenase mechanism has always been assumed to proceed via a Criegee rearrangement mechanism, although the acyl group is a relatively poor migrating group for 1,2-migration reactions. It is known that Baeyer–Villiger oxidation of 1,2-diketones proceeds

- (1) Bugg, T. D. H. *Tetrahedron* **2003**, 59, 7075–7101.
- (2) Que, L., Jr.; Ho, R. Y. N. *Chem. Rev.* **1996**, 96, 2607–2624.
- (3) Bugg, T. D. H.; Lin, G. *Chem. Commun.* **2001**, 941–952.
- (4) Pau, M. Y. M.; Davis, M. I.; Orville, A. M.; Lipscomb, J. D.; Solomon, E. I. *J. Am. Chem. Soc.* **2007**, 129, 1944–1958.
- (5) Spence, E. L.; Langley, G. J.; Bugg, T. D. H. *J. Am. Chem. Soc.* **1996**, 118, 8336–8343.
- (6) Kovaleva, E. G.; Lipscomb, J. D. *Science* **2007**, 316, 453–457.

- (7) Mendel, S.; Arndt, A.; Bugg, T. D. H. *Biochemistry* **2004**, 43, 13390–13396.
- (8) Yamahara, R.; Ogo, S.; Masuda, H.; Watanabe, Y. *J. Inorg. Biochem.* **2002**, 88, 284–294.
- (9) Lin, G.; Reid, G.; Bugg, T. D. H. *J. Am. Chem. Soc.* **2001**, 123, 5030–5039.
- (10) Bruijninx, P. C. A.; Lutz, M.; Spek, A. L.; Hagen, W. R.; Weckhuysen, B. M.; van Koten, G.; Gebbink, R. J. M. K. *J. Am. Chem. Soc.* **2007**, 129, 2275–2286.

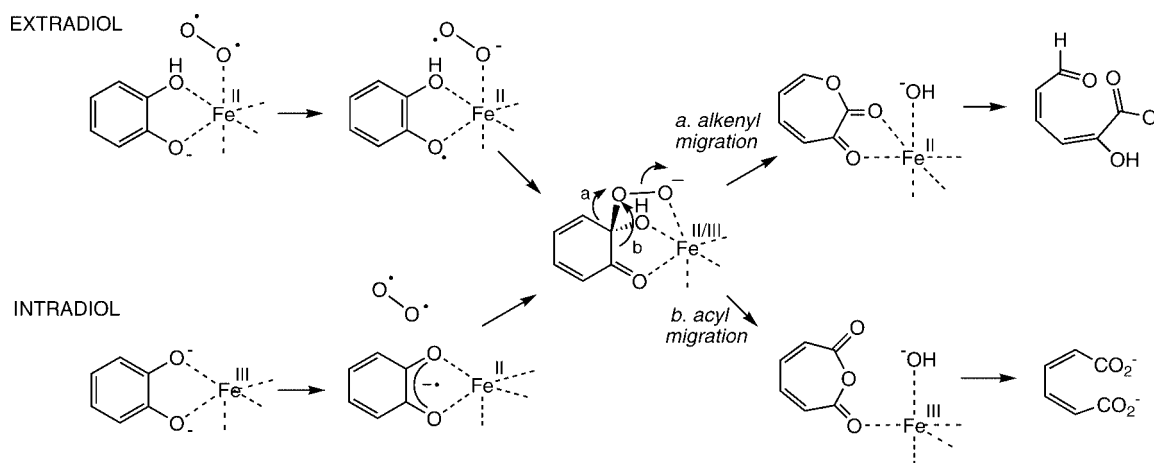


Figure 1. Mechanistic convergence and divergence of the extradiol and intradiol catechol dioxygenase mechanisms, via processing of a common proximal hydroperoxide intermediate.

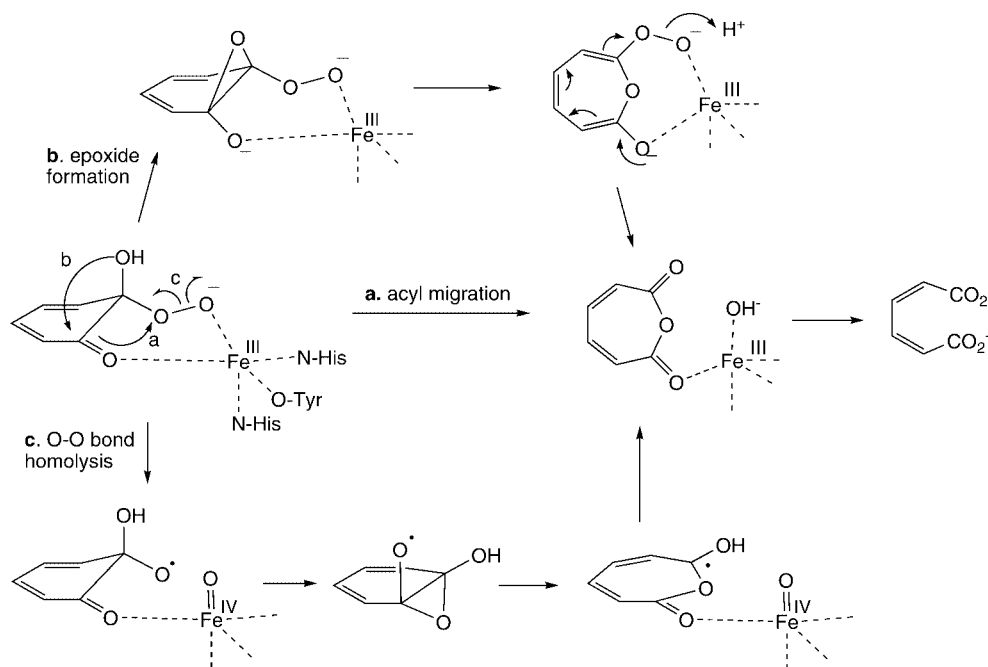


Figure 2. Three possible mechanisms for 1,2-acyl migration reaction during intradiol dioxygenase cleavage: (a) direct 1,2-acyl migration, (b) epoxide formation, followed by benzene oxide-oxepin ring opening, and (c) O—O bond homolysis. In the case of path c, there is an alternative radical mechanism involving β -scission to form an acyl radical; however, recyclization to form muconic anhydride would be needed, since muconic anhydride is a known intermediate.^{1,2}

via 1,2-acyl migration of a similar hydroperoxide intermediate;¹¹ however, isotope labeling studies have shown that precise mechanism of this reaction may not proceed via a direct 1,2-shift.¹² There are two further mechanisms for 1,2-acyl migration, shown in Figure 2: a mechanism involving O—O bond homolysis, for which precedent exists in reactions of alkyl hydroperoxides with iron salts,¹³ and a mechanism involving a benzene oxide-oxepin ring opening, for which we have previously found a chemical precedent.¹⁴ Modeling of the intradiol cleavage reaction catalyzed by protocatechuate 3,4-dioxygenase has been carried out using hybrid DFT methods by Borowski and Siegbahn, who found that the

lowest energy pathway in their model proceeded via a Criegee rearrangement, but that a pathway involving O—O homolytic cleavage could under some circumstances compete with an activation energy 2.2 kcal/mol higher.¹⁵ In this study, we designed and investigated three mechanistic probes to distinguish between these mechanisms, which we tested against catechol 1,2-dioxygenase (CatA) from *Acinetobacter* sp.; ADP1, an enzyme whose three-dimensional structure has been determined;¹⁶ and 2,3-dihydroxyphenylpropionate 1,2-dioxygenase (MhpB) from *Escherichia coli*, an extradiol catechol dioxygenase enzyme that we have previously studied.^{5,7}

Results

Mechanistic Probe 6-Hydroxymethyl-6-methylcyclohexa-2,4-dienone. We previously synthesized carba analogues of the proximal hydroperoxide reaction intermediate, based on substituted cyclohexane skeletons, which acted as inhibitors for

- (11) Krow, G. R. *Org. React.* **1993**, *43*, 251–798.
- (12) Cullis, P. M.; Arnold, J. R. P.; Clarke, M.; Howell, R.; De Mira, M.; Naylor, M.; Nicholls, D. *Chem. Commun.* **1987**, 1088–1089.
- (13) Schreiber, S. L. *J. Am. Chem. Soc.* **1980**, *102*, 6163–6165.
- (14) Eley, K. L.; Crowley, P. J.; Bugg, T. D. H. *J. Org. Chem.* **2001**, *66*, 2091–2097.

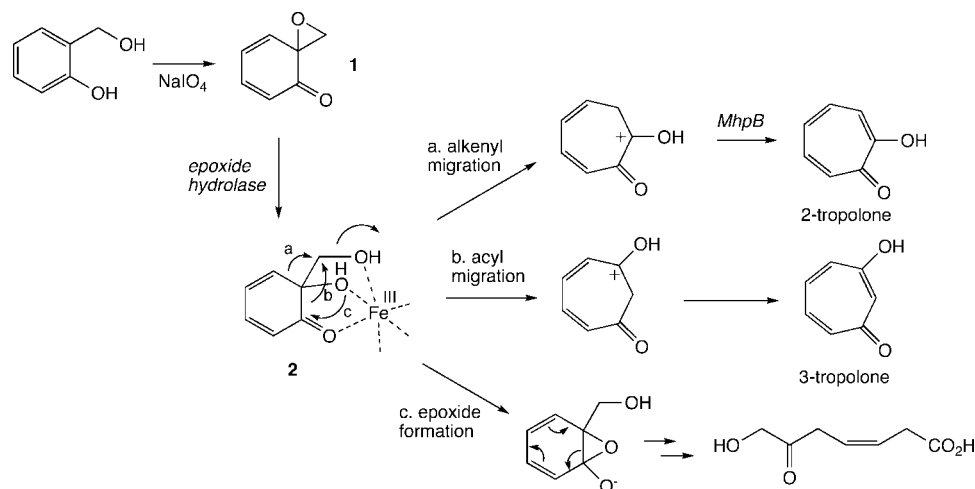


Figure 3. Anticipated reaction products from enzymatic processing of mechanistic probe **2** via 1,2-acyl migration, 1,2-alkenyl migration, or epoxide formation mechanisms.

extradiol dioxygenase MhpB.¹⁷ In this study, we prepared the corresponding carba analogue on the basis of a cyclohexa-2,4-dienone skeleton. The 1,1-spiroepoxy cyclohexadienone (**1**) was prepared by NaIO₄ oxidation of salicyl alcohol, following literature procedures.¹⁸ Treatment of **1** with commercially available *Aspergillus niger* sp. epoxide hydrolase was found to generate the corresponding diol (**2**), which, although rather unstable, was observed as a discrete peak by reverse-phase HPLC at a retention time 18.5 min and was characterized by NMR spectroscopy and mass spectrometry.

Diol **2** represents an interesting mechanistic probe to investigate possible rearrangement mechanisms, since 1,2-alkenyl migration (via a pinacol-type reaction) would generate a 1,2-tropolone product, whereas 1,2-acyl migration would generate a 1,3-tropolone product. Diol **2** is not able to undergo O—O homolytic cleavage but should be able to undergo the benzene oxide—oxepin rearrangement, which would yield an acyclic carboxylic acid product (Figure 3).

Catechol 1,2-dioxygenase (CatA) from *Acinetobacter* sp. ADP1 was expressed and purified as previously described.¹⁹ Incubation of diol **2** with purified CatA gave no new product by HPLC analysis, even after overnight incubation with enzyme. However, incubation of **2** with extradiol dioxygenase MhpB from *E. coli* rapidly formed a bright pink reaction product. Analysis of the silylated reaction product by GC–MS identified the reaction product as 2-tropolone, with identical retention time and fragmentation to authentic 2-tropolone. Complexes of 2-tropolone with iron salts are known to be brightly colored,²⁰ accounting for the formation of the pink color observed. No formation of 1,3-tropolone or acyclic reaction products was detected by HPLC or GC–MS analysis.

Diol **2** was also incubated with iron complexes that are known to catalyze catechol cleavage reactions. No reaction product was observed upon incubation with the iron(III) complex of nitrilo-

triacetic acid,²¹ known to effect intradiol cleavage. However, formation of 2-tropolone was detected upon incubation with iron(II) and iron(III) complexes of 1,4,7-triazacyclononane in methanol, conditions that are known to effect extradiol cleavage.⁹ The formation of 2-tropolone is consistent with the 1,2-alkenyl migration reaction believed to occur in the extradiol reaction mechanism, and the lack of product with CatA indicates a difference in mechanism.

Mechanistic Probe 3-Chloroperoxybenzoic Acid. The second mechanistic probe, designed to investigate a possible O—O bond homolysis mechanism in CatA, is the stable peracid 3-chloroperoxybenzoic acid (MCPBA). If O—O bond homolysis occurs upon ligation to iron(III), then the resulting carboxyl radical will rapidly decarboxylate²² to form a 3-chlorophenyl radical, which upon recombination with an iron(IV)-oxo intermediate would give 3-chlorophenol, as shown in Figure 4. Incubation of MCPBA with *Acinetobacter* CatA for 10 min resulted in the formation of two new reaction products by HPLC analysis, shown to be 2-chlorophenol (RT 19.6 min) and 3-chlorophenol (RT 20.5 min) in a 9:1 ratio. The identity of the reaction products was confirmed by GC–MS analysis and comparison with authentic standards. Extended incubation with CatA for 2 h resulted in the same two products, but in an 8:2 ratio of 2-chlorophenol to 3-chlorophenol. The rates of product formation over 10 min were calculated from HPLC peak heights as 16.1 μmol/min/mg protein for 2-chlorophenol and 1.8 μmol/min/mg protein for 3-chlorophenol, compared with a specific activity of 8.5 μmol/min/mg protein for catechol. Thus, the processing of MCPBA occurs 2-fold faster than *k*_{cat} for catechol.

Incubation of MCPBA with *E. coli* MhpB resulted in the formation of the same products, but with 3-chlorophenol as the major product, in a 9:1 ratio of 3- and 2-chlorophenol. The same products were observed upon treatment of MCPBA with the iron(II) salt of 1,4,7-triazacyclononane, in a ratio of 3:1, respectively, while no product formation was observed with Fe(III)TACN or Fe(III)NTA. In these reactions, a new species at *m/z* 281 was also detected by GC–MS, whose fragmentation pattern is consistent with the structure of a dimeric peroxy ester, shown in Figure 4.

(15) Borowski, T.; Siegbahn, P. E. M. *J. Am. Chem. Soc.* **2006**, *128*, 12941–12953.

(16) Vetting, M. W.; Ohlendorf, D. H. *Structure* **2000**, *8*, 429–440.

(17) Winfield, C. J.; Al-Mahrizy, Z.; Gravestock, M.; Bugg, T. D. H. *J. Chem. Soc., Perkin Trans. 1* **2000**, 3277–3289.

(18) Adler, E.; Brasen, S.; Miyake, H. *Acta Chem. Scand.* **1971**, *25*, 2055–2069.

(19) Strachan, P. D.; Freer, A. A.; Fewson, C. A. *Biochem. J.* **1998**, *333*, 741–747.

(20) Pietra, F. *Chem. Rev.* **1973**, *73*, 293–364.

(21) Weller, M. G.; Weser, U. *Inorg. Chim. Acta* **1985**, *107*, 243–245.

(22) Newcomb, M. *Tetrahedron* **1993**, *49*, 1151–1176.

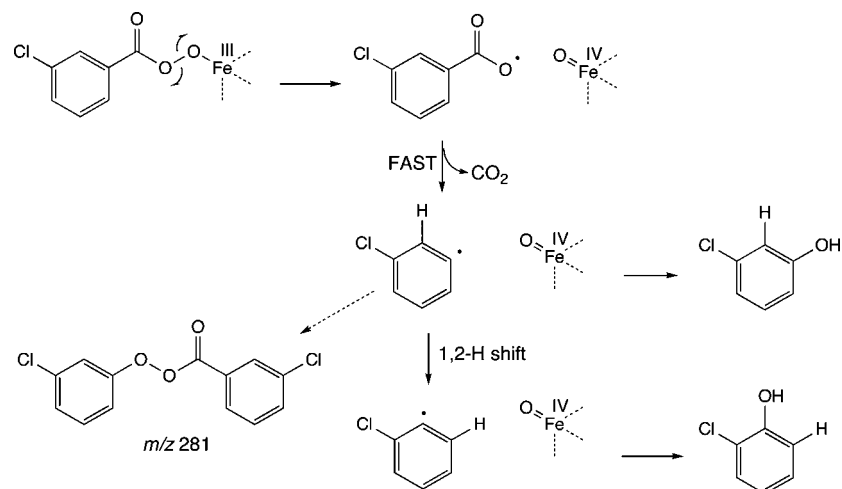


Figure 4. Processing of 3-chloroperoxybenzoic acid via O—O homolytic cleavage mechanism to form the observed 2- and 3-chlorophenol reaction products. The proposed structure of a dimeric byproduct is also shown.

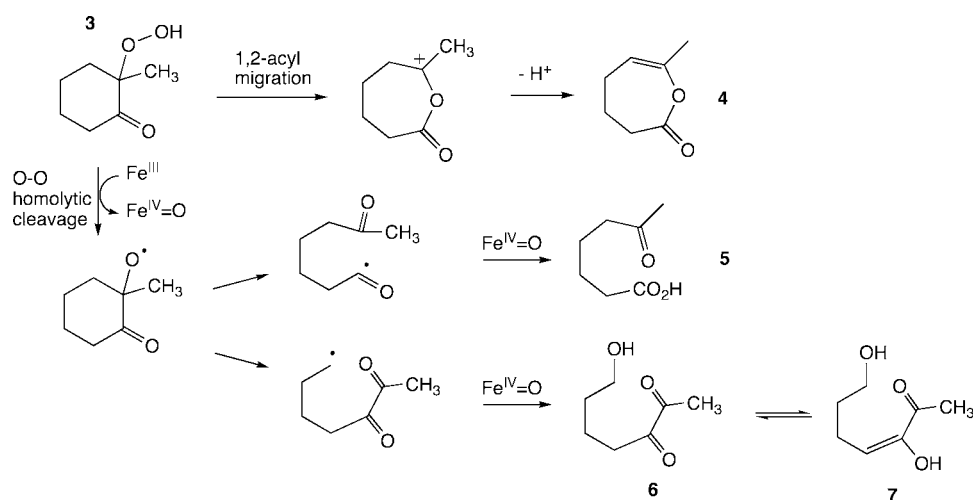


Figure 5. Anticipated reaction products from enzymatic processing of mechanistic probe **3** via 1,2-acyl migration or O—O bond homolysis mechanisms.

The formation of 2- and 3-chlorophenol from MCPBA by intradiol dioxygenase CatA is consistent with the ability to catalyze O—O bond homolysis. The formation of 2-chlorophenol implies that an unusual isomerization has taken place. Since no hydroxylated benzoic or perbenzoic acid products were detected by GC–MS analysis, we believe that the mechanism proceeds via a 3-chlorophenyl radical intermediate, which isomerizes to a 2-chlorophenyl radical via an apparent 1,2-H shift, as shown in Figure 4; however, the precise mechanism of this 1,2-shift has yet to be determined. 2-Chlorophenol is only seen as the major product in the incubation with CatA. O—O bond homolysis products are also observed using extradiol dioxygenase MhpB, and with complexes of iron(II) with tridentate ligand TACN, but not with tetradentate ligand NTA, indicating that O—O bond homolysis can be carried out by iron(II) and (III) salts, but that the coordination state of the iron center is important.

Incubation of 2-Hydroperoxy-2-methylcyclohexanone with Intradiol Dioxygenase CatA. 2-Hydroperoxy-2-methylcyclohexanone (**3**) is a stable hydroperoxide that can be prepared by oxygenation of 2-methylcyclohexanone²³ and contains a car-

bonyl group adjacent to a hydroperoxide and is therefore able to undergo 1,2-acyl migration. This compound therefore allows us to compare the O—O bond homolysis vs acyl migration reaction pathways with an intradiol catechol dioxygenase. The possible reaction products arising from 1,2-acyl migration or O—O homolytic cleavage are illustrated in Figure 5. 1,2-Migration, followed by elimination, would generate an unsaturated lactone (**4**). O—O homolytic cleavage would generate an alkoxy radical, which would undergo C—C fragmentation of an adjacent C—C bond. Oxygenation of the resulting radical would generate either 6-ketoheptanoic acid (**5**) or 5,6-diketoheptan-1-ol (**6**), depending on which C—C bond cleaves.

Incubation of 2-hydroperoxy-2-methylcyclohexanone with CatA for 30 min led to the formation of a strongly UV-absorbent peak at retention time 4.4 min by HPLC analysis. At longer reaction times, this polar reaction product disappeared, and a new peak at retention time 59.1 min was formed, with λ_{max} 323 nm, as shown in Figure 6. Inspection of the possible reaction products in Figure 5 reveals only one that has a conjugated system that would be expected to be UV absorbent: the enol tautomer **7** of 5,6-diketoheptan-1-ol.

To confirm the structure of this species, an independent chemical synthesis was undertaken, as illustrated in Scheme 1.

(23) Cubbon, R. C. P.; Hewlett, C. J. *Chem. Soc. C* **1968**, 24, 2978–2982.

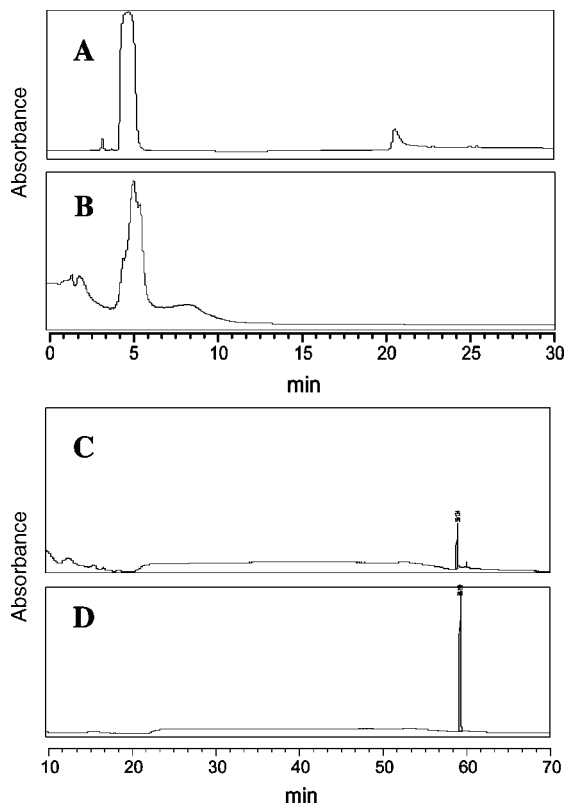
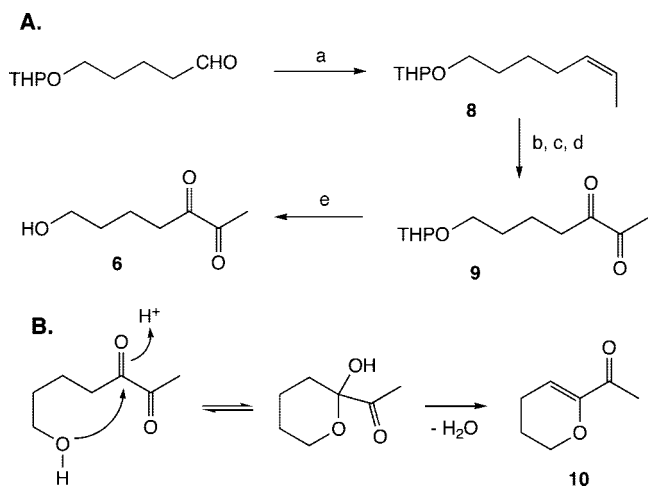


Figure 6. HPLC analysis of reaction products formed by processing compound **3** with CatA after 10 min (A) and 30 min (C), compared with synthetic standard **6** (B, D). (A) Incubation of compound **3** with Cat A (10 min, 220 nm). (B) Synthetic compound **6** (immediate injection, 220 nm). (C) Incubation of compound **3** with CatA (30 min, 320 nm). (D) Synthetic compound **6**, incubated in pH 7.5 buffer (30 min, 320 nm).

Scheme 1^a



^a (a) $\text{EtPh}_3\text{P}^+\text{I}^-$, NaH, 34%. (b) MCPBA, CH_2Cl_2 . (c) NaOH/ H_2O . (d) Pyridinium chlorochromate, CH_2Cl_2 . (e) Silica gel, yield 15% for steps b–e.

Wittig reaction of ethylphosphonium iodide with a THP-protected aldehyde gave alkene **8** as a 2:1 mixture of *Z/E* isomers. The alkene was epoxidized by MCPBA, then converted to the corresponding diol using NaOH, followed by oxidation of the diol to the diketone **9** with pyridinium chlorochromate. Purification of the reaction product by silica column chromatography led to the partial deprotection of the THP protecting group, yielding the target alcohol **6** directly.

Analysis of **6** by reverse-phase HPLC showed very similar behavior to the CatA reaction product: in aqueous solution a peak was initially observed at 4.4 min, followed by formation of a peak at 59.1 min, as shown in Figure 6. Our interpretation of the HPLC data is that, in both cases, cyclization of the free alcohol (**6**) occurs rapidly in aqueous solution, as observed in monosaccharide chemistry, to form the six-membered hemiketal, which can eliminate to form a cyclic enol ether **10**, as shown in Scheme 1B. HRMS analysis of the peak at 59.1 min gives molecular ion 127.0773, consistent with molecular formula $\text{C}_7\text{H}_{10}\text{O}_2$, consistent with the structure of **10**.

The identical retention times and UV–vis spectra of the synthetic sample confirm the identity of the product from reaction with CatA. The formation of this product is consistent with an O–O homolysis reaction pathway, while none of the possible products arising from direct 1,2-acyl migration were detected by HPLC or GC–MS analysis. The rate of conversion of probe **3** by CatA was estimated from the rate of disappearance of **3** by HPLC as $44 \mu\text{mol}/\text{min}/\text{mg}$ of protein. Thus, **3** is processed 5-fold faster than k_{cat} for catechol (specific activity $8.5 \mu\text{mol}/\text{min}/\text{mg}$ of protein).

2-Hydroperoxy-2-methylcyclohexanone (**3**) was also incubated with 1,4,7-triazacyclononane/ FeCl_2 in methanol. Under these conditions, a different reaction product was observed by HPLC analysis, which was identified by NMR and MS analysis as 6-ketoheptanoic acid (**5**), another possible reaction product arising from O–O homolytic cleavage (Figure 5). None of the diketone **6** product was detected in this reaction, and none of the methyl ester of 6-ketoheptanoic acid (**5**) was observed, which could be formed by methanolysis of **4**.

Discussion

Three mechanistic probes were used to investigate three possible mechanisms for the 1,2-acyl migration step of the intradiol catechol dioxygenases. The first mechanism (path a, Figure 2) involves a direct 1,2-acyl migration. Mechanistic probes **2** and **3** are both able to undergo 1,2-rearrangements via acyl migration, **2** via a pinacol rearrangement (migration onto carbon), and **3** via a Criegee rearrangement (migration onto oxygen), but none of the reaction products expected from 1,2-acyl migration were observed in either case.

The second possible mechanism (path c, Figure 2) involves O–O bond homolysis, generating an alkoxy radical, which then undergoes a radical-mediated rearrangement. The transformation of 3-chloroperoxybenzoic acid to a mixture of 2- and 3-chlorophenol by CatA is consistent with a radical mechanism initiated by O–O bond homolysis. However, only the CatA products contained a majority of the 2-chlorophenol product, arising from an apparent 1,2-aryl H shift. The mechanism of this 1,2-shift reaction is intriguing and will be the subject of future studies. The reaction of percarboxylic acids with heme or nonheme iron centers has been studied previously, and it is known that mechanisms involving either homolytic or heterolytic cleavage of the O–O bond of the peracid are possible, depending on the nature of the iron center.²⁴ The same products were isolated from incubations with extradiol dioxygenase MhpB and from some model iron(II) and iron(III) complexes, implying that O–O bond homolysis can be effected by iron(II) or iron(III) complexes, as is known from the chemical literature.¹³ A recent article by Ray et al. shows that O–O bond

(24) Balasubramanian, P. N.; Bruce, T. C. *J. Am. Chem. Soc.* **1986**, *108*, 5495–5503.

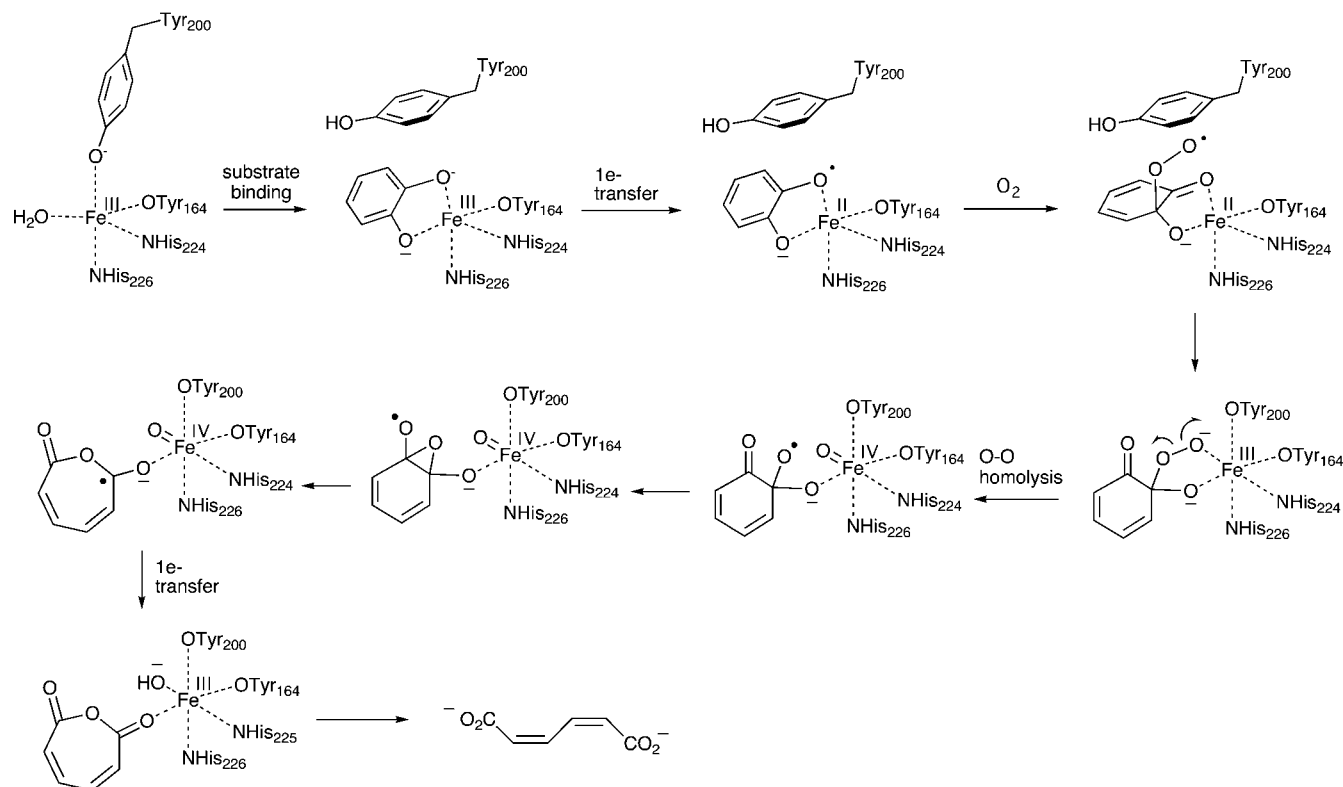


Figure 7. Proposed mechanism for intradiol dioxygenase CatA via O–O homolytic cleavage mechanism. It is not certain whether axial tyrosine-200 remains detached from the iron(III) center in the later steps of the mechanism or becomes reattached (as drawn).

homolysis in MCPBA is favored by complexation to iron(III), whereas complexation by iron(II) favors O–O bond heterolysis, consistent with our data.²⁵

The conversion of 2-hydroperoxy-2-methylcyclohexanone (**3**) to 5,6-diketoheptan-1-ol (**6**) by CatA is also consistent with an O–O bond homolysis pathway and not with 1,2-acyl migration. Incubation of 2-hydroperoxy-2-methylcyclohexanone with FeCl₂ and 1,4,7-triazacyclononane in methanol, conditions used for a biomimetic extradiol cleavage reaction,⁹ resulted in the formation of 2-ketoheptanoic acid (**5**), which is the other expected product arising from O–O bond homolysis (Figure 5), resulting from cleavage of the acyl C–C bond, rather than the alkyl C–C bond. It is interesting that different radical fragmentations occur under different conditions. Cleavage of α -acylalkoxy radicals to acyl radicals is preceded in the literature,²⁶ whereas cleavage to form a less stable primary carbon-centered radical would appear to be a less favorable fragmentation (Figure 5). Therefore, it is likely that the transient iron-oxo species present in the CatA active site is positioned close to the site of the primary radical that is formed, so that C–C cleavage is concerted with C–O bond formation. The observation of a unique O–O bond homolysis product using CatA is consistent with an O–O homolysis mechanism in the CatA reaction mechanism.

The third possible mechanism involves the formation of a benzene oxide intermediate, followed by electrocyclic ring opening (path b, Figure 2). If this mechanism were operating in CatA, then one would expect the carba analogue 6-hy-

droxymethyl-6-methylcyclohexa-2,4-dienone (**2**) to be transformed into an acyclic carboxylic acid product; however, no such product was observed. Therefore, this mechanism seems very unlikely.

Taken together, these results imply that CatA is able to catalyze O–O bond homolysis on mechanistic probes that are structurally related to the hydroperoxide intermediate involved in intradiol catechol cleavage, at reaction rates that are 2–5-fold higher than k_{cat} for the natural substrate catechol, but it is unable to catalyze a direct 1,2-acyl migration. The results therefore support a catalytic mechanism involving O–O bond homolysis, as shown in Figure 7. This conclusion is apparently at odds with previous theoretical studies by Lehnert et al., who found a significant activation energy barrier for O–O homolytic cleavage in a high-spin (TPA)Fe^{III}–OOR complex,²⁷ whereas the corresponding low-spin iron(III) complex is readily able to undergo O–O homolytic cleavage.²⁸ However, modeling studies on the protocatechuate 3,4-dioxygenase reaction mechanism by Borowski and Siegbahn revealed that ligand Tyr-408 is able to assist O–O homolysis via single electron transfer; hence, the activation energy for O–O homolytic cleavage was only 2.2 kcal/mol higher than that for the Criegee rearrangement pathway.¹⁵ The latter study assumed a protonation of the proximal oxygen atom by a bound water molecule,¹⁵ which will assist the Criegee rearrangement pathway. Our experimental results are not consistent with a direct Criegee rearrangement; therefore, further modeling studies on these mechanisms might reveal the effects that the precise geometry of the hydroperoxide complex and the positioning of active-site residues have on the O–O

(25) Ray, K.; Lee, S. M.; Que, L., Jr. *Inorg. Chim. Acta* **2008**, *361*, 1066–1069.

(26) Chatgililoglu, C.; Crich, D.; Komatsu, M.; Ryu, I. *Chem. Rev.* **1999**, *99*, 1991–2069.

(27) Lehnert, N.; Ho, R. Y. N.; Que, L., Jr.; Solomon, E. I. *J. Am. Chem. Soc.* **2001**, *123*, 12802–12816.

(28) MacFaul, P. A.; Ingold, K. U.; Wayner, D. D. M.; Que, L., Jr. *J. Am. Chem. Soc.* **1997**, *119*, 10594–10598.

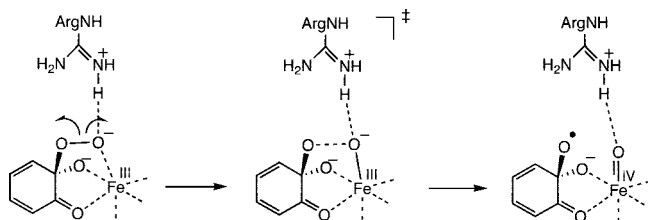


Figure 8. Possible role of arginine-221 in stabilizing the transition state for O—O homolytic cleavage.

homolysis versus Criegee rearrangement pathways. Evidence in favor of an O—O bond homolysis mechanism in model intradiol cleavage reactions has been reported by Hitomi et al., via study of substituent effects and solvent dependence.²⁹

Extradiol dioxygenase enzyme MhpB, in contrast, processed 6-hydroxymethyl-6-methylcyclohexa-2,4-dienone (**2**) into 2-tropolone, via a pinacol rearrangement involving a 1,2-alkenyl migration. This is entirely consistent with the expected Criegee rearrangement mechanism for extradiol dioxygenase cleavage, which is believed to occur through 1,2-alkenyl migration, assisted by acid–base catalysis.^{3,7} The different processing of probe **2** by CatA and MhpB provides a clear difference in behavior between an intradiol and an extradiol catechol dioxygenase. The ring expansion of **2** to a tropolone is of possible relevance to natural product biosynthesis, since there are a number of tropolone natural products whose biosynthesis may proceed via such a ring expansion reaction.³⁰

The implication of this work is that, having formed a proximal hydroperoxide intermediate, the choice of intradiol vs extradiol ring cleavage pathways is ultimately determined by a difference in hydroperoxide rearrangement mechanism. The 1,2-alkenyl migration of the extradiol dioxygenases requires stereoelectronic positioning of the hydroperoxide group, relative to the cyclohexadienone ring,^{3,6} and also requires acid–base catalysis by active-site residues.⁷ The 1,2-acyl migration of the intradiol dioxygenases appears to be mediated by O—O bond homolysis, which might explain why there are no additional acid–base residues in the intradiol dioxygenase active site. What factors might promote O—O bond cleavage, versus other possible reaction pathways? Higher Lewis acidity of the iron(III) center, which is known to favor intradiol cleavage activity in model systems,³¹ would assist bond cleavage, and/or stabilization of the iron(IV) oxo species that is thereby formed. There is a conserved arginine residue in the active site of intradiol dioxygenases studied to date: Arg-221 in the catechol 1,2-dioxygenase structure (PDB file 1DLT) is positioned 3.0–3.8 Å above the bound catechol substrate and 4.0 Å from the iron(III) center.¹⁶ The close proximity of this conserved arginine residue to the bound substrate suggests that it has a role in catalysis, but its precise function is not known. In a catalytic mechanism involving O—O homolytic cleavage, this arginine residue might assist O—O bond homolysis by stabilization of the anionic transition state and/or by stabilization of the transient iron (IV)-oxo species formed, as illustrated in Figure 8. A precedent for this proposal is the distal arginine residue found

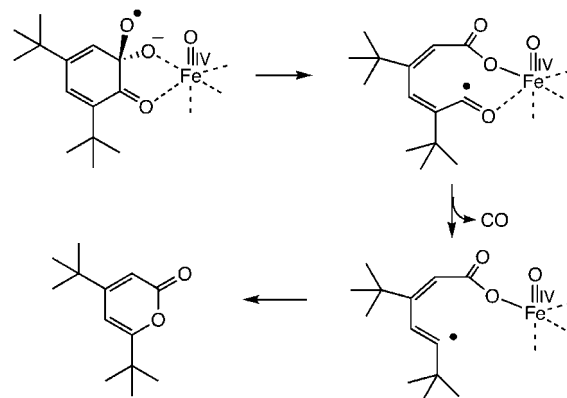


Figure 9. Possible radical mechanism for formation of pyrone catechol cleavage products from 2,4-ditert-butylcatechol.

in the active site of heme peroxidases, which is known to assist O—O bond cleavage and stabilize the iron (IV)-oxo species.³²

Finally, we note that the existence of a radical-based O—O cleavage mechanism that can operate on the proximal hydroperoxide intermediate offers a possible alternative mechanism for the formation of pyrone products observed in several model studies with facial tridentate iron(II) complexes, using 3,5-ditert-butylcatechol as substrate.⁸ It has been proposed that the pyrone products arise from loss of CO from the extradiol α -ketolactone intermediate;³³ however, such a decarbonylation reaction occurring on a stable lactone would be mechanistically very unusual. In contrast, acyl radicals are known to readily decarbonylate to form the corresponding alkyl radical.²⁶ A possible radical mechanism for pyrone formation is shown in Figure 9, whereby, in the presence of the two bulky *t*-butyl substituents and when ligated in a certain conformation, the alkoxy radical formed upon O—O homolysis undergoes C—C homolytic cleavage to form an acyl radical. Decarbonylation of the acyl radical, followed by ring closure, could lead to the formation of the observed pyrone product.

In conclusion, these experiments indicate that the Criegee rearrangements that operate in the intradiol and extradiol catechol dioxygenases occur via quite different mechanisms. The 1,2-alkenyl migration occurring in the extradiol dioxygenases requires acid catalysis and a facial tridentate iron(II) center, and it is assisted by stereoelectronic factors; whereas the observed results suggest that the 1,2-acyl migration occurring in the intradiol dioxygenases operates via a homolytic O—O cleavage mechanism.

Experimental Section

Materials. The *Acinetobacter* sp. ADP1 *catA* gene was subcloned from plasmid pBAC557 (gift of Dr. N. Ornston) using restriction enzymes *Bam*HI and *Spe*I into a pZErO vector (Invitrogen). 6-Hydroxymethyl-6-methylcyclohexa-2,4-dienone (**2**) was prepared by the method of Adler et al.¹⁸ 2-Hydroperoxy-2-methylcyclohexanone (**3**) was prepared by the method of Cubbon and Hewlett.²³

Synthesis of 5,6-Diketohexan-1-ol. 2-(Hept-5-enyloxy)-tetrahydro-2H-pyran (8**).** 5-(Tetrahydro-2H-2-yloxy)pentanal was prepared by conversion of 1,5-pentanediol to the mono-THP ether,

(29) Hitomi, Y.; Yoshida, H.; Tanaka, T.; Funabiki, T. *J. Mol. Catal. A: Chem.* **2006**, *251*, 239–245.

(30) Bentley, R. *Nat. Prod. Rep.* **2008**, *25*, 118–138.

(31) Que, L., Jr.; Kolanczyk, R. C.; White, L. S. *J. Am. Chem. Soc.* **1987**, *109*, 5373–5380.

(32) Hiner, A. N. P.; Raven, E. L.; Thorneley, R. N. F.; Garcia-Canovas, F.; Rodriguez-Lopez, J. N. *J. Inorg. Biochem.* **2002**, *91*, 27–34.

(33) Funabiki, T.; Mizoguchi, A.; Sugimoto, T.; Tada, S.; Tsugi, M.; Sakamoto, H.; Yoshida, S. *J. Am. Chem. Soc.* **1986**, *108*, 2921–2932.

using the procedure of Khan et al.,³⁴ then oxidation using the procedure of Reetz et al.,³⁵ in 58% overall yield. Dry DMSO (100 mL) was deoxygenated with N₂ for 30 min. Sodium hydride (60% dispersion in mineral oil, 2.85 g, 71.0 mmol) was added, and the mixture was heated at 75 °C for 5 min, then cooled to room temperature. Ethyltriphenylphosphonium bromide (26.0 g, 70.0 mmol) was added portionwise, and the mixture was stirred for 45 min. 5-(Tetrahydro-2H-2-yloxy)pentanal (4.7 g, 25.0 mmol) was then added, resulting in an exothermic reaction, which was stirred for 30 min. The reaction mixture was then taken up in water (250 mL) and extracted into ether (3 × 100 mL). After removal of solvent at reduced pressure, the residue was distilled under vacuum to give **8** as a light yellow oil (1.7 g, 8.6 mmol, 34% yield). ¹H and ¹³C NMR analysis showed a mixture of E and Z isomers in ratio of 3:1.

Data: *R*_f 0.31 (2:1 petroleum ether/ethyl acetate). ¹H NMR (400 MHz, CDCl₃) δ_H: 1.60 (3H, d, *J* = 6.0 Hz, CH₃–C=C), 1.35–1.45 (2H, m), 1.50–1.65 (6H, m), 1.65–1.72 (1H, m), 1.7–1.85 (1H, m), 2.66 (2H, q, *J* = 7.3 Hz, –CH₂–C=C), 3.39 and 3.74 (2 × 1H, m, THP CH₂O), 3.50 and 3.86 (2 × 1H, m, CH₂O), 4.58 (1H, t, *J* = 1.5 Hz, THP acetal CHO), 5.3–5.49 (2H, m, CH=CH) ppm. ¹³C NMR (100 MHz, CDCl₃) δ_C: 12.7 and 15.5 (Z/E isomers), 19.5, 22.8, 25.7, 28.9, 30.7, 32.3, 62.6, 67.5, 98.83, 123.9, and 124.9 (Z/E isomers), 130.4 and 131.3 (Z/E isomers) ppm. HRMS: *m/z* 221.1507 (MNa⁺), calcd 221.1512 for C₁₂H₂₂O₂Na.

7-Hydroxyheptane-2,3-dione (6). To a solution of 2-(hept-5-enyloxy)-tetrahydro-2H-pyran (100 mg, 0.50 mmol) in dichloromethane (5 mL) was added MCPBA (120 mg, 0.7 mmol), and the reaction was stirred for 1 h. Removal of solvent at reduced pressure gave the epoxide product as a light yellow oil (98 mg, *m/z* (ESI, +ve): 237 [M + Na]⁺). The epoxide product was then dissolved in distilled water (10 mL), and 1 M NaOH (1 mL) was added. After being stirred for 48 h, the reaction mixture was extracted into diethyl ether. The organic layer was dried (Na₂SO₄) and evaporated to give the diol product (255 [M + Na]⁺). The residue was then dissolved in dichloromethane (10 mL) at room temperature, to which was added pyridinium chlorochromate (600 mg), and the mixture was stirred for 3 days. The reaction mixture was washed with water and dried (Na₂SO₄), and the solution was concentrated in vacuo. The product was purified by column chromatography, eluting with petroleum ether/ethyl acetate (6:1). 7-Hydroxyheptane-2,3-dione (**6**) was eluted directly from the column (*R*_f 0.1, petroleum ether/ethyl acetate, 6:1) and was obtained as a colorless oil (20 mg, 15% yield). ¹H NMR (400 MHz, *d*₆-acetone) δ_H: 1.84 (2H, qui, *J* = 6.0 Hz), 1.90 (2H, qui, *J* = 6.0 Hz), 2.02 (3H, s, CH₃CO–), 2.56 (2H, t, *J* = 7.0 Hz, –CH₂CO–), 4.33 (2H, t, *J* = 5.8 Hz, –CH₂OH). ¹³C NMR (100 MHz, *d*₆-acetone) δ_C: 19.1, 22.3, 25.1, 29.9, 69.5, 198.9, 199.2 ppm. HRMS: *m/z* 127.0773 ([MH–H₂O]⁺), calcd 127.0754 for C₇H₁₁O₂.

Incubation of Mechanistic Probes with *Acinetobacter* CatA. CatA from *Acinetobacter* sp. ADP1 was expressed from *E. coli* Top10/pZERocatA by induction with 0.5 mM IPTG at OD₆₀₀ = 0.6 and purified using the method of Strachan et al.¹⁹ to give an enzyme of specific activity 8.6 U/mg. Incubations with CatA were carried out in 50 mM Tris/HCl buffer (pH 7.5, 100 mL), containing either (A) 6-hydroxymethyl-6-hydroxycyclohexa-2,4-dienone **2** (NMR data given below), generated by treatment of spiroepoxy-2,4-cyclohexadienone **1** (10 mM) with 5 mg of *Aspergillus niger* epoxide hydrolase for 30 min, (B) 10 mM 3-chloroperoxybenzoic acid, or (C) 10 mM 2-hydroperoxy-2-methylcyclohexanone **3**. To each incubation was added 800 μL (15 units) of CatA enzyme.

Aliquots (5 mL) were removed after 10, 60, 90, 180 min, and 48 h, and the reaction was stopped by adding 300 μL of 100% trichloroacetic acid (TCA) after 10, 60, 90, 180 min, and 48 h,

respectively. The samples were centrifuged for 10 min at 13000 rpm and then analyzed by HPLC on a Phenomenex Luna C₁₈ reverse-phase column. The mobile phase consisted of A (100% water) and B (100% methanol) delivered at a flow rate of 0.8 mL/min. The gradient program was 5% B (5 min); 5–100% B (15 min); 100% B (3 min); and 100–5% B (7 min). HPLC retention times: spiroepoxide **1**, 3.7 min; 6-hydroxymethyl-6-hydroxycyclohexa-2,4-dienone **2**, 18.6 min; 3-chlorophenol, 20.5 min; 2-chlorophenol, 18.6 min; synthetic 7-hydroxyheptane-2,3-dione (**6**), 4.4 min; enol ether **10**, 59.1 min. Spectroscopic data for 6-hydroxymethyl-6-hydroxycyclohexa-2,4-dienone **2** (400 MHz, D₂O) δ_H: 3.69 and 3.83 (2H, 2 × d, *J* = 9.0 Hz, –CH₂OH), 6.08 (2H, m, H-2 and H-5), 6.79 (1H, dt, *J* = 9.5, 3.5, 3.5 Hz, H-4), 6.86 (1H, dt, *J* = 9.5, 5.8, 5.8 Hz, H-3) ppm. ¹³C NMR (100 MHz, D₂O) δ_C: 69.3, 92.3, 116.3, 121.1, 128.3, 134.5, 201.6 ppm. ESI-MS: [MNa]⁺ = 163.

Incubation of Mechanistic Probes with *E. coli* MhpB. *E. coli* MhpB was overexpressed from a recombinant plasmid pIPB containing the *mhpB* gene (gift of Dr. J. L. Garcia, CSIC, Madrid), in *E. coli* strain DH5α. Overproduction of MhpB was induced by addition of IPTG (0.5 mM) to a 2-L culture of *E. coli* DH5α/pIPB in Luria broth containing 100 μg/mL of ampicillin at OD₆₀₀ = 0.6, followed by growth at 37 °C for 4 h. Following cell lysis, MhpB was purified to near homogeneity by hydrophobic interaction chromatography, as previously described,³⁶ using 50 mM potassium phosphate (pH 7.0) containing 0.07% (v/v) β-mercaptoethanol as buffer.

Incubations with MhpB were carried out in 50 mM potassium phosphate buffer (pH 8.0, 100 mL), containing either (A) 6-hydroxymethyl-6-hydroxycyclohexa-2,4-dienone, generated by treatment of spiroepoxy-2,4-cyclohexadienone solid (10 mM) with 5 mg of *Aspergillus niger* epoxide hydrolase for 30 min or (B) 10 mM 3-chloroperoxybenzoic acid. To each incubation was added 400 μL (30 units) of MhpB enzyme, which had been preactivated by addition of ammonium iron(II) sulfate (5 mM) and sodium ascorbate (5 mM) for 1 min at 0 °C.

Aliquots (5 mL) were removed after 10, 60, 90, 180 min, and 48 h, and the reaction was stopped by adding 300 μL of 100% TCA after 10, 60, 90, 180 min, and 48 h, respectively. The samples were centrifuged for 10 min at 13000 rpm and then analyzed by HPLC on a Phenomenex Luna C₁₈ reverse-phase column. The mobile phase consisted of A (100% water) and B (100% methanol) delivered at a flow rate of 0.8 mL/min. The gradient program was 5% B (5 min); 5–100% B (15 min); 100% B (3 min); 100–5% B (7 min). Samples for GC–MS analysis were extracted into HPLC-grade dichloromethane, and the organic layer was dried with Na₂SO₄. A portion of the product was treated with *N,O*-bis(trimethylsilyl)acetamide (200 μL) and chlorotrimethylsilane (10 μL) overnight and then diluted with HPLC-grade dichloromethane and analyzed by GC–MS under electron impact mode using a Micro-mass Autospec GC–MS system Varian 4000 (at 70 eV) on a DB5 silica capillary column by using the following temperature gradient: 50 °C for 1 min, 50–140 at 25 °C min^{–1}, and 140–250 at 5 °C min^{–1}. Data for 2-tropolone (TMS derivative): retention time 6.64 min, *m/z* 194.2 (MH⁺, 40%), 180.2 (100%).

Incubation of Mechanistic Probes with Biomimetic Iron Complexes. Iron(III) Nitrilotriacetate Model Reaction. Mechanistic probes were incubated at 10 mM concentration under the conditions described by Weller and Weser,²¹ in the presence of 40 mM Fe(ClO₄)₃ and 40 mM NTANa₃ in 0.3 M borate buffer pH 8.0, for 5 days at room temperature. Products were analyzed by HPLC or GC–MS, with derivatization as described above.

Iron(II) 1,4,7-Triazanonane Model Reaction. Mechanistic probes were incubated at 1.02 mM concentration under the conditions described by Lin et al.,⁹ in the presence of 0.2 mM FeCl₂, 0.2 mM 1,4,7-triazacyclononane, and 0.6 mM pyridine in methanol for 48 h at room temperature. Products were analyzed by HPLC or GC–MS, with derivatization as described above. Data for 6-keto-

(34) Khan, A. T.; Ghosh, S.; Choudhury, L. H. *Eur. J. Org. Chem.* **2005**, 4891–4896.

(35) Reetz, M. T.; Drewes, M. W.; Schwickardi, R. *Org. Synth.* **1999**, 76, 110.

(36) Bugg, T. D. H. *Biochim. Biophys. Acta* **1993**, 1202, 258–264.

heptanoic acid (**5**): ^1H NMR (400 MHz, d_6 -acetone) 1.52–1.59 (4H, m), 2.08 (3H, s, $-\text{CH}_3$), 2.29 (2H, t, $J = 7.2$ Hz, $-\text{CH}_2\text{COCH}_3$), 2.47 (2H, t, $J = 7.2$ Hz, $-\text{CH}_2\text{COOH}$) ppm. ^{13}C NMR (100 MHz, d_6 -acetone) 23.9, 25.1, 29.8, 33.9, 43.3, 177.2, 207.9 ppm. MS (ESI-MS, +ve): 183 ($[\text{M} + \text{K}]^+$, 10%), 167 ($[\text{M} + \text{Na}]^+$, 100%) HRMS: obsd 167.0681 for MNa^+ , calcd 167.0679 for $\text{C}_7\text{H}_{12}\text{O}_3\text{Na}$.

Acknowledgment. We thank Prof. L. N. Ornston (Yale University) for the gift of plasmid pBAC557 containing the *Acinetobacter* sp. *catA* gene, Dr. Kirstin Eley (University of

Warwick) for the gift of the pZErOcatA construct, and Dr. John Bickerton (University of Warwick) for assistance with GC–MS experiments.

Supporting Information Available: HPLC and GC–MS data for each of the incubations of the three mechanistic probes with dioxygenases CatA and MhpB and under nonenzymatic model reaction conditions. This material is available free of charge via the Internet at <http://pubs.acs.org>.

JA8029569